Bioorganic & Medicinal Chemistry Letters 23 (2013) 3262–3266

Contents lists available at SciVerse ScienceDirect

Bioorganic & Medicinal Chemistry Letters

journal homepage: www.elsevier.com/locate/bmcl

Conformation constraint of anilides enabling the discovery of tricyclic lactams as potent MK2 non-ATP competitive inhibitors

Dong Xiao [a,*], Anandan Palani [a], Xianhai Huang [a], Michael Sofolarides [a], Wei Zhou [a], Xiao Chen [a], Robert Aslanian [a], Zhuyan Guo [b], James Fossetta [c], Fang Tian [c], Prashant Trivedi [c], Peter Spacciapoli [d], Charles E. Whitehurst [d], Daniel Lundell [c]

[a] Medicinal Chemistry, Merck Research Laboratories, 2015 Galloping Hill Road, Kenilworth, NJ 07033, USA
[b] Chemical Modeling & Informatics, Merck Research Laboratories, 2015 Galloping Hill Road, Kenilworth, NJ 07033, USA
[c] In vitro Pharmacology, Merck Research Laboratories, 2015 Galloping Hill Road, Kenilworth, NJ 07033, USA
[d] In vitro Pharmacology & Oncology, Merck Research Laboratories, 33 Avenue Louis Pasteur, Boston, MA 02115, USA

ARTICLE INFO

Article history:
Available online 4 April 2013

Keywords:
Conformation constraint
Alkyl anilide conformation
Non-ATP competitive MK2 inhibitors

ABSTRACT

Conformation restriction of linear *N*-alkylanilide MK2 inhibitors to their *E*-conformer was developed. This strategy enabled rapid advance in identifying a series of potent non-ATP competitive inhibitors that exhibited cell based activity in anti-TNFα assay.

The anti-TNFα (tumor necrosis factor α) biologics introduced in the late 1990s have generated a much needed breakthrough in the treatment of several autoimmune diseases such as rheumatoid arthritis (RA), Crohn's disease and psoriasis.[1] The huge commercial success of etanercept (Enbrel®), infliximab (Remicade®) and adalimumab (Humira®) provided prove of concept and incentives for the search of new therapeutic interventions using small molecules based on TNFα antagonism.[2] During the last decade, p38 inhibition has emerged as one of the potential approaches. The p38 mitogen-activated protein kinase (MAPK) pathway has been implicated in the regulation of mRNA stability of TNF-α, along with many other targets, which could be inhibitory or stimulatory immune mediators.[3] Several p38 inhibitors have entered clinical trials, however, due to either broad and complex effects on immunoresponses or exposure limited by safety factors, p38 inhibition did not translate into sufficient clinical benefits.[4] Alternative approaches by inhibition at different points in the pathway, therefore, have been investigated. MAPK-activated protein kinase 2 (MK2)[5] is one of the most important downstream targets of p38. It has been proposed that inhibition of the MK2 kinase would result in the reduction of TNF-α production.[6] Targeting MK2 not only could afford more selectivity, it also would avoid other p38 mediated pathways that may be stimulatory, therefore, may improve clinical efficacy. In animal models, a recent report showed that MK2 knockout mice were viable and devoid of rheumatoid arthritis.[7] These findings prompted industry-wide discovery research on MK2 inhibitors.[8]

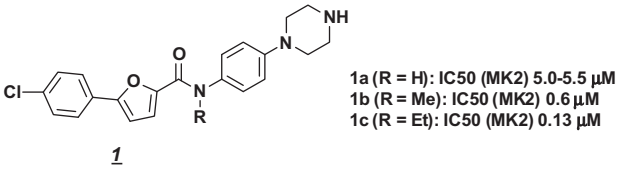

1

Figure 1. Linear MK2 non-ATP competitive inhibitors.

We recently reported the discovery of a series of non-ATP competitive MK2 inhibitors **1**.[9] (Fig. 1) They were discovered by affinity selection-mass spectrometry-based screening[10] against an MK2 construct in the presence of 100 mM ATP. Compared with previously known ATP competitive inhibitors, the non-competitive mode of inhibition may have several advantages. Since they do not bind in the active site, they usually have improved selectivity vs. other kinases. Additionally, cellular ATP (2–5 mM) with high affinity to P38α MAPK-activated MK2 (K_M = 2 μM)[11] would not compete with these inhibitors, making it easier to achieve inhibitory efficacy. The initial lead series was considered a good starting point for lead optimization of the medicinal chemistry program. Subsequently, compound **1a** had been subject to preliminary SAR investigation on the amide NH. It was shown that the alkylated analogs such as **1b** and **1c** exhibited significantly increased potency (Fig. 1).[9]

* Corresponding author.
E-mail address: dong.xiao@merck.com (D. Xiao).

0960-894X/$ - see front matter © 2013 Elsevier Ltd. All rights reserved.
http://dx.doi.org/10.1016/j.bmcl.2013.03.109

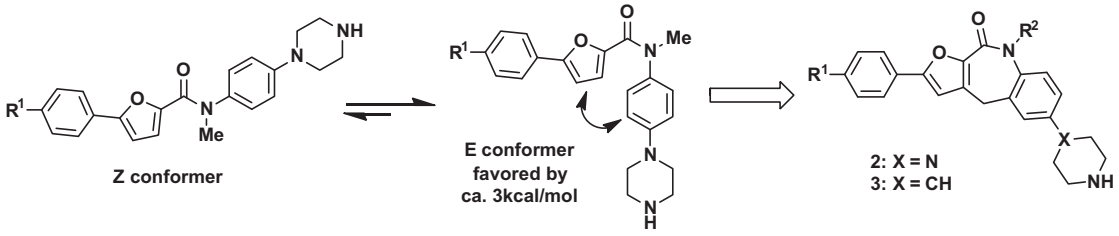

Scheme 1.

At the inception of this lead optimization program, we decided to introduce conformational constraint to the linear system **1**. This could not only benefit compound potency in general but also reveal new avenues for synthetically incorporating side chain novelty.

From a design point of view, we were intrigued by the pronounced effects of amide *N*-alkyl groups and speculated that it was a result of conformational change of the amide bond. It was reported in the literature that alkylanilides exist in a conformation favoring the *E*-conformer by 2–3 kcal/mol over *Z*-conformer.[12] This led to our design of targets such as **2** to constrain the system with a methylene bridge between furan and *N*-phenyl group (Scheme 1). We were also interested in replacing the piperazine moiety with a piperidine **3**. This would decrease electron density on the phenyl ring it is attached to and would likely reduce Ames issue liabilities as predicted by Multicase software.[13]

The chemical synthesis of novel furan-fused tricycles **2**/**3** was challenging. Through extensive experimentation, we discovered an approach via tri-substituted furan intermediates using metallation chemistry.[14] Thus, when commercial **4** was treated Knochel-type mixed piperidine base followed by addition to aldehyde **5**, the desired product **6** was obtained in 60–70% yield. Upon reduction of the nitro group, the carbinol was activated and was reduced by triethylsilane/TFA to yield **7**. The lactamization to **8** was achieved using LHMDS, which was further elaborated to final analogs **2** by alkylation and deprotection (Scheme 2).

The synthesis of piperidine analog **3** took a different approach due to availability of starting material. Commercial alkynyl boronic ester **9** was treated with Schwartz reagent followed by transmetallation with $ZnCl_2$ then Pd-catalyzed coupling[15] with iodide **10** to afford **11**. Subsequent Suzuki coupling with **12** generated **13**, which was cyclized using LHMDS. The alkene **14** was cleaved by

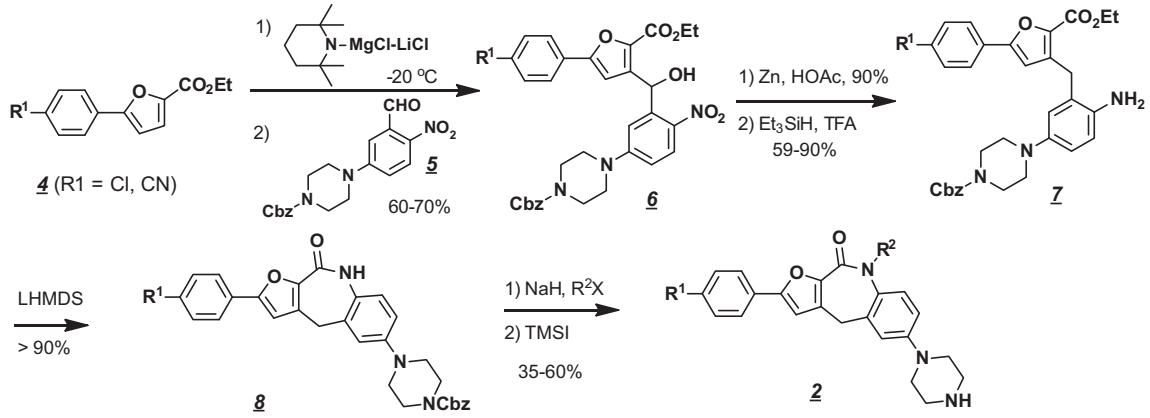

Scheme 2.

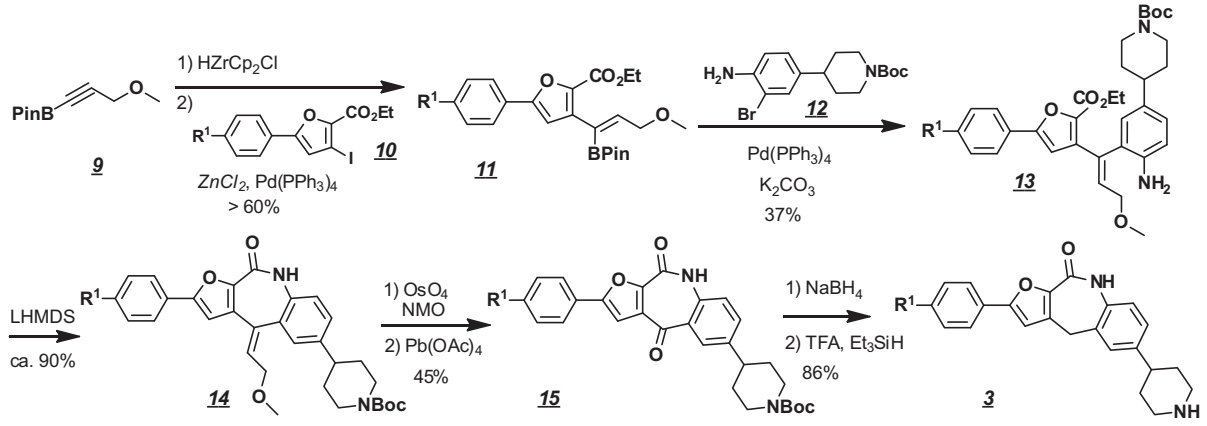

Scheme 3.

Table 1
MK2 inhibition[16] data of tricyclic analogs

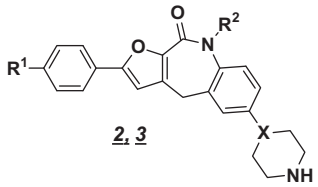

2, 3

Entry	R^1	R^2	x	IC_{50} (MK_2) (nM)
2a	—Cl	—H	N	96
2b	—Cl	—	N	79
2c	—Cl		N	12
2d	—Cl		N	110
2e	—Cl	—F, F	N	107
2f	—Cl	N	N	64
2g	—Cl	Br	N	52
2h	—CN	—H	N	110
3a	—Cl	—H	CH	14
3b	—CN	—H	CH	28

Data represented the average values of duplicates or triplicates.

OsO_4/NMO followed by treatment of $Pb(OAc)_4$ to afford ketone **15**. Additional manipulation using $NaBH_4$ then Et_3SiH/TFA, the two step reduction/deprotection protocol, furnished the final compounds **3** (Scheme 3).

The data generated from testing **2** and **3** were shown in Table 1. In the piperazine series, the unsubstituted lactam **2a** showed 50 fold increase in potency over linear analog **1a**. Furthermore, unlike the linear series, in which the N-methylated **1b** boosted the potency nine-fold over **1a**, N-methylated **2b** showed similar activity to **2a**. Taking together, these results confirmed our speculation that the drastic change of potency in the linear series between NH and *N*-alkyl amides was due to the conformational change. The resulting *E*-alkylanilide was indeed the active conformation. The remarkable potency improvement from **1a** to **2a** validated our design strategy and demonstrated the power of conformational constraint. Additionally, the piperidine series of analogs **3a** and **3b** were even more potent.

Upon establishment of the viability of tricyclic lactam as a novel MK2 scaffold, and completion of initial investigation of alkyl and aryl groups, our attention turned to *N*-biaryl substitution, that was shown to significantly enhance potency in the linear series.[17] In the piperazine series, the desired analogs were conveniently synthesized by Suzuki coupling of key Cbz protected bromide **2g** (an intermediate obtained in Scheme 2) followed by deprotection of piperazine nitrogen using TMSI to complete analogs **2i–2s** (Scheme 4).

The corresponding biaryl analogs in the piperidine series were synthesized through a different pathway. Thus, compound **14** was alkylated with 2-bromobenzylbromide to afford **16**. Further elaboration to cleave the trisubstituted olefin was best achieved using OsO_4/NMO followed by $Pb(OAc)_4$. At this point, Suzuki reactions on compound **17** were used to install the desired biaryl groups. Finally, the resulting ketone **18** was reduced to methylene analog **3c** by $NaBH_4$ then Et_3SiH/TFA sequence. We were also interested in the difluoro-analog **3d** which could block potential metabolism[18] at the methylene bridge. This compound was synthesized by treating ketone **18** with deoxofluor® to afford **19** followed by deprotection using TFA (Scheme 5).

From the data shown in Table 2, the biaryl substituted tricyclic lactams indeed proved to be very potent analogs. The potency of chloro- and cyano-analogs (**2n** vs **2o** and **2r** vs **2s**) were quite similar. The difference between piperidine and piperazine analog **2s** and **3c** was not as pronounced as in the unsubstituted series. The most potent compounds all bore some polar atoms/groups on the distal aryl ring, with bis-*meta* substitutions affording <10 nM activity. Interestingly, the difluoro analog **3d** also maintained potency, indicating the methylene position could be a useful venue for potential further functionalization.

The most potent compound **2s** was further profiled. In the cell-based biochemical assay, using a MK2 downstream target HSP27[19] in THP-1 cells, **2s** showed EC_{50} of 138 nM. It was also active in inhibiting LPS-stimulated hTNFα with EC_{50} of 150 nM.[20] In addition, this compound was tested in the MK2 enzyme assay in the presence of 1 and 100 μM ATP where Cheng–Prusoff equation would predict an approximate 35-fold shift in IC_{50} for an ATP competitive inhibitor, but as shown in Figure 2 no shift in potency was observed. This was consistent with the tricyclic series retaining the non-ATP competitive characteristics of the progenitor linear series.

It is noteworthy that the tricyclic lactams **2** and **3** were generally not cytotoxic, with CC_{50} of **2f** at 17.4 μM in the SW1353 toxicity assay, greater than 270-fold of its MK2 IC_{50}. The tricyclic series also retained the high kinase selectivity as existed in the progenitor linear series. For example, the test screen of **2n** on an in-house kinase selectivity panel shows the excellent selectivity retained against 21 sampled kinases (Table 3).

In summary, we presented a useful strategy of constraining linear anilides which enabled the discovery of a novel series of tricyclic lactams as MK2 inhibitors. These MK2 inhibitors exhibited excellent cell based activities with desired non-ATP competitive characteristics. They were not cytotoxic and showed good kinase selectivity. Our design strategy may be broadly applicable in alkylanilide containing amide bond conformational control. This conformational approach also led to a novel chemical patent space securing freedom of operation.

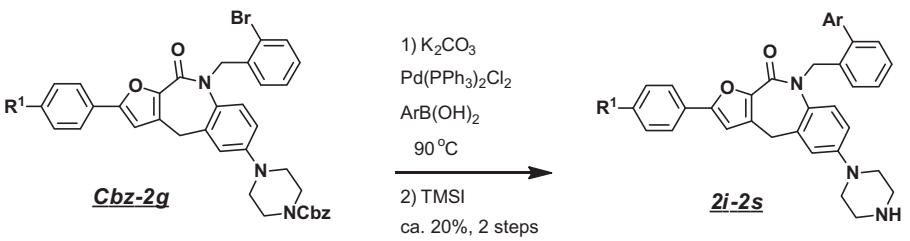

Scheme 4.

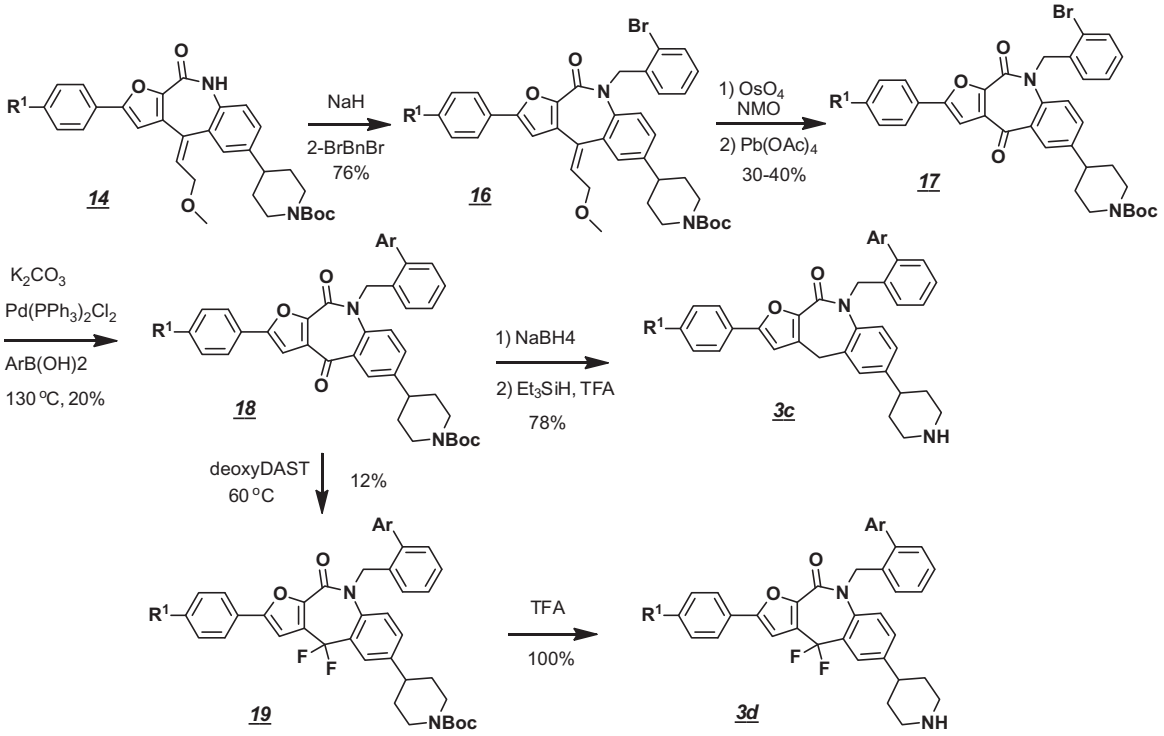

Scheme 5.

Table 2
MK2 assay data of biaryl tricyclic lactam analogs

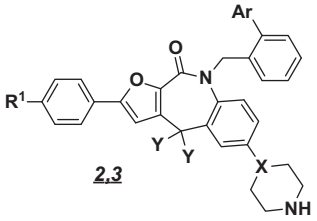

2,3

Entry	R^1	Ar	X	Y	IC_{50} (MK_2) (nM)
2i			N	H	74
2j			N	H	14
2k		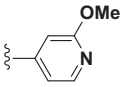	N	H	21
2l		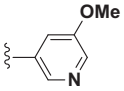	N	H	4.9
2m			N	H	39
2n			N	H	22
2o			N	H	21
2p			N	H	8.4

Table 2 (*continued*)

Entry	R^1	Ar	X	Y	IC_{50} (MK_2) (nM)
2q			N	H	6.8
2r			N	H	5.7
2s			N	H	1.9
3c			CH	H	3.0
3d			CH	F	8.9

Data represented the average values of duplicates or triplicates.

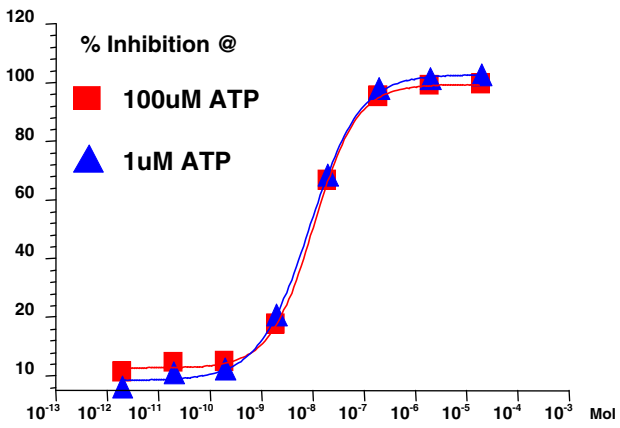

Figure 2. Inhibition data of compound **2s** in different ATP concentrations.

Table 3
In-house kinase screening data of **2n**

Kinase	FLT3	PLK3	CSNK1D	NEK2	PKCA	IRAK4	AKT1	IKKB	ROCK2	JAK2	CAMK4
IC_{50} (μM)	>30	>30	>30	13.0	10.0	26.0	16.0	24.0	>20	11.0	27.0
Kinase	MET	IGF1R	EGFR	LCK	MST2	ERK2	CHK1	TSSK2	EPHB4	GSK3B	
IC_{50} (μM)	>30	>30	>30	>19	>12	>30	>18	>30	>30	>30	

Acknowledgments

The authors thank Drs. Malcolm MacCoss and William Greenlee for stimulating discussions and supports of this research program and Dr. Nigel Liverton for valuable comments and editions on this Letter.

References and notes

1. Mousa, S. A.; Goncharuk, O.; Miller, D. *Expert Opin. Biol. Ther.* **2007**, *7*, 617.
2. (a) Palladino, M. A.; Bahjat, F. R.; Theodorakis, E. A.; Moldawer, L. L. *Nat. Rev. Drug Disc.* **2003**, *2*, 717; (b) Reimold, A. M. *Curr. Drug Targets Inflammation Allergy* **2002**, *1*, 377.
3. (a) Schindler, J. F.; Monahan, J. B.; Smith, W. G. *J. Dent. Res.* **2007**, *86*, 800; (b) Saklatvala, J. *Curr. Opin. Pharmacol.* **2004**, *4*, 372; (c) Kumar, S.; Boehm, J.; Lee, J. C. *Nat. Rev. Drug Disc.* **2003**, *2*, 717.
4. (a) Sweeney, S. E. *Nat. Rev. Rheumatol.* **2009**, *5*, 475; (b) Schett, G.; Zwerina, J.; Firestein, G. *Ann. Rheum. Dis.* **2008**, *67*, 909.
5. (a) Hitti, E.; Iakovleva, T.; Brook, M.; Deppenmeier, S.; Gruber, A. D.; Radzioch, D.; Clark, A. R.; Blackshear, P. J.; Kotlyarov, A.; Gaestel, M. *Mol. Cell. Biol.* **2006**, *26*, 2399; (b) Gaestel, M.; Mengel, A.; Bothe, U.; Asadullah, K. *Curr. Med. Chem.* **2007**, *14*, 2214.
6. (a) Dean, J. L.; Sully, G.; Clark, A. R.; Saklatvala, J. *Cell. Signal.* **2004**, *16*, 1113; (b) Tietz, A. B.; Malo, A.; Diebold, J.; Kotlyarov, A.; Herbst, A.; Kolligs, F. T.; Brandt-Nedelev, B.; Halangk, W.; Gaestel, M.; Goeke, B.; Schaefer, C. *Am. J. Physiol.* **2006**, *290*, G1298.
7. Hegen, M.; Gaestel, M.; Nickerson-Nutter, C. L.; Lin, L.-L.; Telliez, J.-B. *J. Immunol.* **2006**, *177*, 1913.
8. For recent reviews on MK2 inhibitors: (a) Schlapbach, A.; Huppertz, C. *Future Med. Chem.* **2009**, *1*, 1243; (b) Duraisamy, S.; Bajpai, M.; Bughani, U.; Dastidar, S. G.; Ray, A.; Chopra, P. *Expert Opin. Ther. Targets* **2008**, *12*, 921.
9. Huang, X.; Shipps, G. W.; Cheng, C. C.; Spacciapoli, P.; Zhang, X.; McCoy, M. A.; Wyss, D. F.; Yang, X.; Achab, A.; Soucy, K.; Montavon, D. K.; Murphy, D. M.; Whitehurst, C. E. *ACS Med. Chem. Lett.* **2011**, *2*, 632.
10. Annis, D. A.; Nickbarg, E.; Yang, X.; Ziebelland, M. R.; Whitehurst, C. E. *Curr. Opin. Chem. Biol.* **2007**, *11*, 518.
11. Mourey, R. J.; Burnette, B. L.; Brustkern, S. J.; Daniels, J. S.; Hirsch, J. L.; Hood, W. F.; Meyers, M. J.; Mnich, S. J.; Pierce, B. S.; Saabye, M. J.; Schindler, J. F.; South, S. A.; Webb, E. G.; Zhang, J.; Anderson, D. R. *J. Pharmacol. Exp. Ther.* **2010**, *333*, 797.
12. Itai, A.; Toriumi, Y.; Saito, S.; Hiroyuki, Kagechika; Shudo, K. *J. Am. Chem. Soc.* **1992**, *114*, 10649.
13. MULTICASE software: Klopman, G. *Quant. Struct.-Act. Relat.* **1992**, *11*, 176. Multicase Inc.: http://www.multicase.com MULTICASE simulation predicted **2a** to be Ames positive in one out of three models, whereas **3a** to be negative in all three models.
14. Krasovskiy, A.; Krasovskaya, V.; Knochel, P. *Angew. Chem., Int. Ed.* **2006**, *45*, 2958.
15. Deloux, L.; Skrzypczak-Jankun, E.; Cheesman, B. V.; Srebnik, M.; Sabat, M. *J. Am. Chem. Soc.* **1994**, *116*, 10302.
16. *MK2 IMAP assay:* All the components of MK2 phosphorylation reaction made are 4× concentrated in 1× reaction buffer containing10 mM Tris, pH 7.2, 10 mM $MgCl_2$, 1 mM DTT, 0.05% azide and 0.01% Tween 20 and the reaction was carried in 384 well black reaction plate at room temperature in dark. Mix 5 μL of 4× inhibitor in 4% DMSO, 5 μL of 400 μM ATP and 5 μL of 200 pM MK2 kinase and incubate for 30 min. Reaction started by adding 5 mL of 400 nM TAMRA labeled peptide and incubating 30 min in dark. The final concentrations are: 1× inhibitor, 1% DMSO, 100 μM ATP, 50 pM MK2 and 100 nM substrate. Reaction was stopped by adding 60 μL of 1:400 diluted Progressive Binding Reagent in 1× Progressive Binding Buffer A and incubating 30 min in dark. Read plate at Analyst HT 96-384 Plate Reader (LJL BioSystem) equipped with Fluorescence Polarization module (Excitation wavelength 530 nm and Emission wavelength 580 nm).
17. Huang, X.; Zhu, X.; Chen, X.; Zhou, W.; Xiao, D.; Degrado, S.; Aslanian, R.; Fossetta, J.; Lundell, D.; Tian, F.; Trivedi, P.; Palani, A. *Bioorg. Med. Chem. Lett.* **2012**, *22*, 65.
18. Metabolism simulation of compound **2a** predicted that the methylene bridge was a major metabolic hot spot. Simulation software: MetaSite 4.0.2 (http://www.moldiscovery.com/index.php, Molecular Discovery Ltd.) Also see: Cruciani, G.; Carosati, E.; De Boeck, B.; Ethirajulu, K.; Mackie, C.; Howe, T.; Vianello, R. *J. Med. Chem.* **2005**, *48*, 6970.
19. *LPS Induced Phospho-HSP27 serine78 assay:* Bring the THP-1 cells to log-phase by passing the cells at proper density a day previous to the assay (1×10^5 cells/mL). Spin to collect cells and suspend in fresh complete-RPMI-1640 medium at cell density of 2.5×10^6 cells/mL. Add equal volume of RPMI-1640 without FBS containing 40 nM Okadaic Acid (final: 100,000 cells/80 μL/well). Plate 100,000 cells/80 μL into flat-bottom cell culture plate and incubate at 37 °C for 60 min. Add 10 μL of 10× diluted-compound in 1% DMSO in 5% FBS-RPMI medium and incubate at 37 °C for 60 min. Add 10 μL of 10× LPS in 5% FBS-RPMI medium and incubate at 37 °C for 60 min. Add 25 μL 5× Cell Lysis Buffer containing 5× Halt Inhibitors and incubate on ice for 30 min. Transfer cell lysate to glass fiber filter plate and stack the filter plate on top of a 96-well storage plate. Spin stacked filter-storage plate at 3500 rpm for 5 min at 4 °C. MesoScale pHSP27 S78 Assay 10–20 μL cell lysate was used in this assay.
20. *Assay of TNFα secretion from THP1 cells:* THP1 cells were obtained from ATCC (Cat. No. TIB-202) and cultured in medium consisting of RPMI1640 supplemented with 2 mM L-glutamine, 1.5 g/L sodium bicarbonate, 4.5 g/L glucose, 10% fetal bovine serum, 10 mM HEPES, 1 mM sodium pyruvate and 50 μM 2-mercapatoethanol. Cells were plated into the wells of 96-well culture plates at 0.5×10^5 cells/well for TNFα, then cultured for 60 min to allow pre-equilibration, and the treated with varying concentrations of compound **2s** for 30 min prior to addition of LPS (Sigma–Aldrich, Cat. No. L2654) at 1 μg/mL. After 3 h of culture for TNFα assays, supernatants were removed and secreted cytokines were measured using commercially available kits and manufacturer's protocols. Secreted TNFα was specifically measured by an ELISA method (R&D Systems; Cat. No. DTA00C).